Journal of Catalysis 377 (2019) 1–12

Contents lists available at ScienceDirect

Journal of Catalysis

journal homepage: www.elsevier.com/locate/jcat

The new role of surface adsorbed $CH_x(x = 1–3)$ intermediates as a co-adsorbed promoter in self-promoting syngas conversion to form CH_x intermediates and C_2 oxygenates on the Rh-doped Cu catalyst

Riguang Zhang [a,b], Cong Wei [a], Debao Li [c], Zhao Jiang [d], Baojun Wang [a,*], Lixia Ling [a], Maohong Fan [b,e,*]

[a] Key Laboratory of Coal Science and Technology of Ministry of Education and Shanxi Province, Taiyuan University of Technology, Taiyuan 030024, Shanxi, PR China
[b] College of Engineering and Applied Science, and School of Energy Resources Engineering, University of Wyoming, Laramie, WY 82071, USA
[c] State Key Laboratory of Coal Conversion, Institute of Coal Chemistry, Chinese Academy of Sciences, Taiyuan 030001, Shanxi, PR China
[d] School of Chemical Engineering and Technology, Xi'an Jiaotong University, Xi'an 710049, PR China
[e] School of Civil and Environmental Engineering, Georgia Institute of Technology, Atlanta, GA 30332, USA

ARTICLE INFO

Article history:
Received 8 May 2019
Revised 8 July 2019
Accepted 9 July 2019

Keywords:
Syngas
C_2 oxygenates
CH_x intermediate
Rh-doped Cu catalyst
Density functional theory

ABSTRACT

Syngas conversion to C_2 oxygenates includes two crucial steps that CO activation to form $CH_x(x = 1–3)$ intermediates, followed by its reaction with CO/CHO to form the C—C chain, in which the $CH_x(x = 1–3)$ intermediates were widely recognized as the reactive intermediates to yield C_2 oxygenates. Inspired by the reported studies about the role of co-adsorbed OH intermediates that promote CO activation and the C—C chain formation in syngas conversion, an idea about the new role of surface adsorbed CH_x intermediates in syngas conversion is proposed, that is, whether the surface adsorbed CH_x intermediates itself also act as a co-adsorbed promoter to self-promote CO activation and conversion. This study revealed for the first time that in syngas conversion to C_2 oxygenates over Rh-doped Cu catalysts, the surface adsorbed $CH_x(x = 1–3)$ intermediates not only act as the reactive intermediates to participate into the reactions with CO/CHO, but also itself act as a self-promoter to facilitate CO activation to form $CH_x(x = 1–3)$ intermediates and promote CHO reaction with $CH_x(x = 1–3)$ to form C_2 oxygenates. Especially, the dominant CH_2 intermediate acted as a co-adsorbed promoter exhibits higher activity and selectivity towards itself formation and C_2 oxygenates CH_2CHO instead of methanol and hydrocarbons, respectively. Moreover, the internal mechanism of surface adsorbed CH_x intermediate is explained from the electronic property aspect. This newly so-called CH_x self-promoting syngas conversion mechanism offers new insights into the fundamental role of surface adsorbed $CH_x(x = 1–3)$ intermediates in CO activation and conversion to form C_2 oxygenates, and open a new mechanism that is likely general and involved in the reactions related to $CH_x(x = 1–3)$ intermediates formation.

© 2019 Elsevier Inc. All rights reserved.

1. Introduction

Syngas ($CO + H_2$) conversion to form C_2 oxygenates (typically such as ethanol) is an important process in the transformation of coal, natural gas, and biomass into higher-value products [1–4]. At present, the complex reaction network, slow kinetics and low selectivity become the major obstacles for syngas conversion to C_2 oxygenates [2]. Up to now, there are generally four types of catalysts in syngas conversion to C_2 oxygenates: Rh-based catalyst [5–9], Mo-based catalyst [10,11], modified F-T synthesis catalyst [12–15], and Cu-based catalyst [16–18], in which the catalytic performance of the catalyst is improved by the bimetallic synergetic mechanism. Among them, Rh-doped Cu-based bimetallic catalysts have attracted much attention for CO activation and carbon-containing species hydrogenation in the past years due to the lower cost and the stronger resistance towards coking compared to the Rh-based catalyst [19]. Experimentally, RhCu alloy catalyst was obtained by a limited miscibility, and the Cu-Rh binary alloy phase diagrams [20–23] found that two alloy phases (Rh-rich and Cu-rich) are formed at T < 1400 K. Rodriguez et al. [24] have investigated Rh deposition on Cu(1 0 0) surface using X-ray Photoelectron Spectroscopy (XPS), and found that Rh centers have a remarkable positive charge. Density functional theory (DFT) studies indicated that the introduction of Cu into Rh or Pd obviously alter CO adsorption ability [25,26]. Zhao et al. [19] discovered that Rh-doped Cu(1 1 1) surface in syngas conversion significantly

* Corresponding authors at: College of Engineering and Applied Science, and School of Energy Resources Engineering, University of Wyoming, Laramie, WY 82071, USA (M. Fan).
E-mail addresses: wangbaojun@tyut.edu.cn, wbj@tyut.edu.cn (B. Wang), mfan@uwyo.edu, mfan3@mail.gatech.edu (M. Fan).

https://doi.org/10.1016/j.jcat.2019.07.019
0021-9517/© 2019 Elsevier Inc. All rights reserved.

lower the barriers of CO reaction with CH_x and improve the selectivity of C_2 oxygenates in comparison with the Rh(1 1 1) surface. Moreover, Rh-doped Cu(2 1 1) surface facilitates the formation of CH_3 and its reaction with CO in comparison with Cu(2 1 1) surface, which exhibits better productivity and selectivity towards ethanol formation [27]. Thus, in this study, Rh-doped Cu bimetallic catalyst is considered for syngas conversion, in which Cu is considered as the main component, and Rh is used as a second metal.

For the mechanism of syngas conversion to form C_2 oxygenates, two crucial steps are generally accepted: one is that CO activation to form key CH_x(x = 1–3) intermediates via the CO direct or H-assisted dissociation mechanism [28], CO is directly dissociated into C, then, C is successively hydrogenated to produce CH_x(x = 1–3) intermediates [27]; alternatively, H-assisted CO dissociation goes through CO hydrogenation to CH_xO(x = 1–3) or CH_xOH (x = 1,2), then, the dissociation of CH_xO(x = 1–3) or CH_xOH(x = 1,2) via the C—O bond breakage to form CH_x(x = 1–3) intermediates; moreover, CH_xO or CH_xOH can also be hydrogenated to form methanol. The second step is CO/CHO reaction with CH_x(x = 1–3) intermediates to produce the C—C bond of C_2 oxygenates [5,19,29–32], in which CH_x intermediate as an important species go through the successive hydrogenation, CO/CHO reaction with CH_x or the coupling of CH_x leading to the formation of methane, C_2 oxygenates or C_2 hydrocarbons, respectively [5,19,27,30–36].

On the basis of above analysis, it is concluded that CH_x(x = 1–3) species acted as the key intermediate can yield C_2 oxygenates. However, along with the formation of CH_x(x = 1–3) over the Rh-, Co- and Cu-based catalysts [5,19,27,30–38], which mainly come from the dissociation of CH_xO(x = 1–3) or CH_xOH(x = 1,2) by its C—O bond breakage, the intermediates such as O and OH species are also produced. Since syngas conversion is carried out under the hydrogen-rich conditions, the produced O or OH species will be hydrogenated to form OH or H_2O. Up to now, extensive studies have investigated the roles of H_2O and OH species in syngas conversion [39–48]. Jiménez-Barrera et al. [44] demonstrated that low concentration of H_2O contributes to CO dissociation on Ru/Al_2O_3 catalyst; Storsæter et al. [45] reported the effect of H_2O on the alumina supported cobalt catalysts, where H_2O irreversibly deactivates the catalyst in the Fischer–Tropsch synthesis. Similarly, the surface OH species is also of great importance for syngas conversion, Schweicher et al. [46] experimentally investigated syngas conversion over Co/MgO catalyst, and confirmed the existence of surface OH species contributes to the formation of carbon chain; Gunasooriya et al. [47] found that CO activation to form the CH species and the carbon chain on Co(1 1 1) surface under the surface OH-assisted is more preferred over that under the surface H-assisted; Zha et al. [48] compared CO activation over Co-doped Cu(1 1 1) surface under the H- and OH-assisted conditions, indicating that the OH-assisted promotes CO hydrogenation to CH_xOH (x = 1,2), followed by its dissociation via the C—O bond cleavage leading to CH_x species.

Based on above analysis, especially inspired by the role of OH species in syngas conversion that promotes CO activation to form the CH_x(x = 1–3) intermediates and facilitates the C—C bond formation, an idea about the new role of surface adsorbed CH_x(x = 1–3) intermediates in syngas conversion is proposed, except for the well-known role of CH_x(x = 1–3) intermediates acted as the reactive species to participate into the reaction with CO/CHO, more importantly, whether the surface adsorbed CH_x(x = 1–3) intermediates can act as a co-adsorbed promoter to self-promote syngas conversion, including CO activation to form CH_x(x = 1–3) species and CO/CHO reaction with CH_x(x = 1–3) to form C_2 oxygenates. Hereafter, we call this new mechanism as CH_x self-promoting syngas conversion mechanism.

In this study, aiming at revealing the new role of surface adsorbed CH_x(x = 1–3) intermediates acted as a co-adsorbed promoter in self-promoting syngas conversion to form C_2 oxygenates, Rh-doped Cu catalysts with four kinds of model surfaces were built to reflect the new role of surface adsorbed CH_x(x = 1–3) intermediates as a co-adsorbed promoter; then, CO activation to form CH_x(x = 1–3) species and the related reaction of CH_x(x = 1–3) species leading to methane, the C—C bond formation of C_2 oxygenates and hydrocarbons are fully examined using the density functional theory (DFT) calculations. Further, the electronic properties including the Bader charge, the differential charge density, density of states, and the *d*-band center were systematically analyzed, which presents the correlation between the electronic property and catalytic performance affected by the new role of surface adsorbed CH_x(x = 1–3) intermediates.

2. Computational details

2.1. Calculation methods

The Vienna Ab-initio Simulation Package (VASP) code was used to perform all DFT calculations in this study [49,50]. We adopt the generalized gradient approximation (GGA) with the exchange-correlation functional Perdew-Burke-Ernzerhof (PBE) [51]. The optimization convergence of three-layers RhCu(1 1 1) surface was checked with the forces less than 0.01 eV·Å^{-1} and the energy difference less than 5×10^{-6} eV, which is also applied in the geometry optimization. On the other hand, the climbing-image nudged elastic band method (CI-NEB) was employed to obtain the transition states for each elementary reaction [52,53]. The dimer method [54,55] was carried out to further optimize the transition states with the convergence criteria of the force acting on the atom less than 0.05 eV Å; then, the energy of the transition state structure is further calculated at the convergence force criteria of 0.01 eV·Å^{-1}. Thus, the calculated energies in this study are all at the convergence force criteria of 0.01 eV·Å^{-1}, which can be well compared among these energy values; meanwhile, the transition state was verified using the single imaginary frequency. Supplementary Material lists the details for calculating relevant energy.

2.2. Surface model

Based on the experiment and theoretical studies [19–27], Rh-doped Cu catalysts is modeled using Rh-doped Cu(1 1 1) surface. For the Rh-doped Cu(1 1 1) surface, as shown in Fig. 1(a), a $p(3 \times 3)$ three-layer supercell Cu(1 1 1) surface was employed with a vacuum slab of 15 Å; then, one surface Cu atom is replaced by one Rh atom, denoted as RhCu(1 1 1). During the calculations, the bottom one layer was fixed to model the bulk positions, while other layers and the adsorbates are allowed to relax. In addition, the three-layer model employed in this study has been widely applied to the reactions of ethanol oxidation, decomposition, synthesis, and methanol formation [56–59]. In addition, in order to further verify the rationality of three-layers Rh/Cu(1 1 1) surface model, the adsorption energies of CO at the top Rh site as the most stable site over the four- and five-layers Rh/Cu(1 1 1) surface models (the bottom one layers are fixed to their bulk positions, and the other top layers and with adsorbates are relaxed) are further calculated. The corresponding adsorption energies of CO are 182.9 and 185.8 kJ·mol^{-1} over the four- and five-layers RhCu(1 1 1) surfaces, respectively, which are close to the value of 183.9 kJ·mol^{-1} over the three-layer RhCu(1 1 1) surface, suggesting that the three-layers RhCu(1 1 1) surface employed in this study is reasonable and reliable to investigate syngas conversion to C_2 oxygenates.

There are four types of adsorption sites (top, bridge, fcc and hcp) over the RhCu(1 1 1) surface, which correspond to nine different sites due to the adsorption site consisted of different types of metal

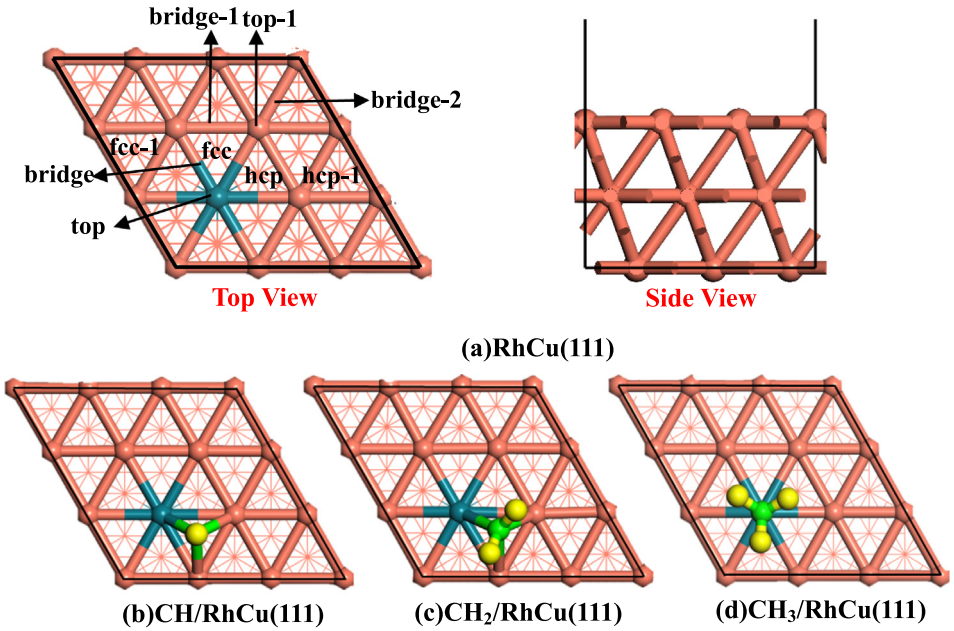

Fig. 1. The surface morphology and adsorption sites of RhCu(1 1 1) and CH_x(x = 1–3)/RhCu(1 1 1) surfaces. Orange, dark green, green and yellow balls correspond to Cu, Rh, C and H atoms, respectively.

atoms, as shown in Fig. 1(a), top, top-1, bridge, bridge-1, bridge-2, fcc, fcc-1, hcp, and hcp-1, respectively.

On the other hand, aiming at identifying the new role of surface adsorbed CH_x(x = 1–3) intermediates as a co-adsorbed promoter over Rh-doped Cu catalysts, as shown in Fig. 1(b)–(d), three types of RhCu(1 1 1) surfaces are constructed using the CH, CH_2 or CH_3 intermediates adsorbed on the clean RhCu(1 1 1) surface, which are named as CH/RhCu(1 1 1), CH_2/RhCu(1 1 1) and CH_3/RhCu (1 1 1) surfaces, respectively.

3. Results and discussions

3.1. CO activation to form CH_x(x = 1–3) intermediates

As mentioned in Introduction, the formation of CH_x(x = 1–3) intermediates via CO direct dissociation hardly occur on the Cu [27,37,38], Rh [30,35,60–62] and Rh-doped Cu(1 1 1) surfaces [27], which mainly comes from H-assisted CO dissociation mechanism. Subsequently, CO/CHO reaction with the dominant CH_x(x = 1–3) monomer leads to C_2 oxygenates. As a result, the formation of CH_x(x = 1–3) intermediates via the mechanism of H-assisted CO dissociation on Rh-doped Cu catalyst is investigated in this study. All possible elementary reactions involving in the formation of CH_x(x = 1–3) intermediates, methane, as well as the C—C bond formation of C_2 oxygenates and hydrocarbons on the RhCu (1 1 1) and CH_x(x = 1–3)/RhCu(1 1 1) surfaces are listed in Table 1. The energy profile of the optimal formation route of CH_x(x = 1–3) and CH_3OH are shown in Figs. 3–5 (see details in Figs. S2–S7).

3.1.1. The adsorption and co-adsorption of key intermediates

The adsorption energy can be used to evaluate the strength between the adsorbates and the catalyst, which plays a crucial role

Table 1
Activation free energy (ΔG_a) and reaction free energy (ΔG) of the elementary reactions involving in the formation of C_2 oxygenates from syngas over the RhCu(1 1 1) and CH_x(x = 1–3)/RhCu(1 1 1) surfaces at 523 K.

Reactions		$\Delta G_a(\Delta G)$/kJ·mol^{-1}			
		RhCu(1 1 1)	CH/RhCu(1 1 1)	CH_2/RhCu(1 1 1)	CH_3/RhCu(1 1 1)
Rx-1	CO + H → CHO	112.9(103.8)	90.3(63.8)	106.1(88.2)	108.7(84.4)
Rx-2	CHO → CH + O	213.8(136.5)	231.5(137.2)	174.2(129.9)	152.9(114.3)
Rx-3	CHO + H → CHOH	84.2(12.2)	72.4(28.4)	80.7(42.0)	80.1(37.9)
Rx-4	CHOH → CH + OH	155.3(65.0)	117.6(68.6)	115.6(41.5)	106.1(22.3)
Rx-5	CHO + H → CH_2O	44.9(20.4)	48.6(27.3)	50.8(33.7)	49.6(15.2)
Rx-6	CH_2O → CH_2 + O	170.7(84.9)	178.8(68.2)	140.1(67.6)	198.0(113.1)
Rx-7	CH_2O + H → CH_2OH	100.6(20.4)	75.3(−2.4)	80.6(−1.3)	85.7(18.4)
Rx-8	CHOH + H → CH_2OH	38.9(−2.0)	38.1(−28.2)	40.6(−15.1)	85.7(−1.1)
Rx-9	CH_2OH → CH_2 + OH	110.6(31.0)	107.6(37.1)	55.1(21.7)	77.9(−1.5)
Rx-10	CH_2O + H → CH_3O	53.6(9.2)	58.8(−17.7)	60.8(−22.8)	59.8(−40.2)
Rx-11	CH_3O → CH_3 + O	141.9(46.0)	163.5(47.4)	174.1(71.6)	167.3(65.6)
Rx-12	CH_3O + H → CH_3OH	100.2(0.4)	57.2(−8.3)	69.6(5.6)	51.2(−14.2)
Rx-13	CH_2OH + H → CH_3OH	33.0(−40.6)	40.0(−34.0)	32.1(−53.2)	37.9(−71.6)
Rx-14	CH_2 → CH + H	50.2(0.1)	85.5(54.8)	84.5(−57.1)	81.4(42.6)
Rx-15	CH_2 + H → CH_3	35.4(−39.8)	45.1(−60.3)	46.0(−48.0)	48.2(−40.6)
Rx-16	CH_3 + H → CH_4	28.6(−52.3)	26.8(−80.4)	26.4(−87.5)	16.1(−97.5)
Rx-17	CH_2 + CH_2 → C_2H_4	43.5(−165.6)	70.4(−138.3)	75.6(−125.3)	36.0(−156.3)
Rx-18	CO + CH_2 → CH_2CO	51.8(4.5)	61.0(4.1)	80.8(23.1)	48.9(−8.9)
Rx-19	CHO + CH_2 → CH_2CHO	31.9(−84.3)	37.6(−72.2)	24.4(−83.2)	5.6(−108.4)

It is noted that the values of x is 1–4 corresponding to the RhCu(1 1 1) and CHx(x = 1–3)/RhCu(1 1 1) surfaces, respectively.

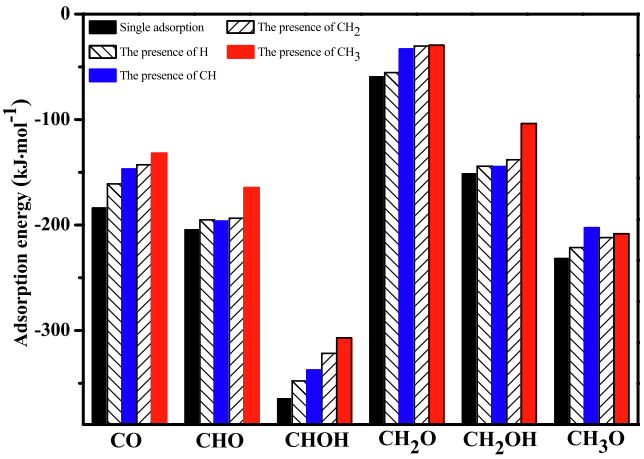

Fig. 2. The adsorption energy of key CO, CHO, CHOH, CH_2OH and CH_3O intermediates in the form of the single adsorption, as well as in the presence of surface adsorbed H, CH, CH_2 and CH_3 intermediate, respectively.

in the catalytic reaction. Up to now, most of the studies only investigate the single adsorption of key intermediates (CO, CHO, CH_2O, CH_3O, CHOH, CH_2OH) in syngas conversion and their co-adsorption with the H, O or OH species [30,48,63,64]. In this study, to gain a better understanding about the new role of surface adsorbed CH_x(x = 1–3) intermediate as a co-adsorbed promoter, the adsorption behaviors of these key intermediates are examined on the RhCu(1 1 1) and CH_x(x = 1–3)/RhCu(1 1 1) surfaces (see details in Fig. S1 and Table S1). The results show that all C_1 species (CO, CHO, CH_2O, CH_3O, CHOH, CH_2OH and CH_3OH) prefer to be located at the top Rh site, Rh-Cu bridge site and the fcc site consisted of a Rh atom and two Cu atoms.

As presented in Fig. 2, compared to the adsorption of single CH_xO(x = 0–3) and CH_xOH(x = 1,2) intermediates, the co-adsorbed H or CH_x(x = 1–3) species decrease the adsorption energy of key intermediates CH_xO(x = 0–3) and CH_xOH(x = 1,2), suggesting that the presence of H or CH_x(x = 1–3) species is favorable for the migration of these key intermediates on RhCu(1 1 1) surface. Moreover, compared to H species, CH_x(x = 1–3) species is more favorable to decrease the adsorption energies of CH_xO(x = 0–3) and CH_xOH (x = 1,2) intermediates, the lateral interactions induced by the presence of CH_x(x = 1–3) species change the adsorption sites of CH_xOH(x = 1,2) and CH_xO(x = 0–3) intermediates, which is similar to that the lower adsorption energy favored the migration of adsorbates among the active sites of catalyst surface [48,64].

3.1.2. CH formation

In the H-assisted CO dissociation mechanism, CH is produced via the dissociation of CHO or CHOH intermediates via the C—O bond breakage. On the clean RhCu(1 1 1) and CH_x(x = 1–3)/RhCu (1 1 1) surfaces, as presented in Fig. 3, CH formation dominantly goes through the route of CO + 2H → CHO + H → CHOH → CH + OH, which have the overall barriers of 271.3, 210.5, 246.7 and 228.4 kJ·mol^{-1}, respectively; they are all endothermic by 181.0, 161.5, 172.6 and 144.6 kJ·mol^{-1}, respectively. Thus, CH_x(x = 1–3)/RhCu(1 1 1) surface is more advantageous to CH formation in kinetics and thermodynamics than the clean RhCu(1 1 1) surface, suggesting that surface adsorbed CH_x(x = 1–3) intermediates acted as the co-adsorbed promoter over RhCu(1 1 1) surface not only promotes syngas conversion to form CH intermediate, but also exhibits different promotion effect towards CH formation with the activity order of CH/RhCu(1 1 1) > CH_3/RhCu(1 1 1) > CH_2/RhCu(1 1 1) > RhCu(1 1 1).

3.1.3. CH_2 formation

CH_2 can be produced by the dissociation of CH_2O or CH_2OH intermediates via the C—O bond cleavage. On the RhCu(1 1 1) and CH_x(x = 1,2)/RhCu(1 1 1) surfaces (see Fig. 4(a)–(c)), the route of CO + H → CHO + H → CHOH + H → CH_2OH → CH_2 + OH is mainly responsible for CH_2 formation, which are endothermic by 145.0, 101.5 and 119.1 kJ·mol^{-1} with the overall barriers of 224.6, 172.0 and 174.8 kJ·mol^{-1}, respectively. Interestingly, on CH_3/RhCu (1 1 1) surface, as presented in Fig. 4(d), the main route is CO + 3H → CHO + 2H → CH_2O + H → CH_2OH → CH_2 + OH, this route is also endothermic by 116.5 kJ·mol^{-1} with the overall barrier of 195.9 kJ·mol^{-1}.

As mentioned above, in comparison with the clean RhCu(1 1 1) surface, CH_x(x = 1–3)/RhCu(1 1 1) surface prefers to form CH_2 in kinetics and thermodynamics, namely, the surface adsorbed CH_x(x = 1–3) intermediates acted as the co-adsorbed promoter also facilitates CH_2 formation, moreover, it change the optimal route of CH_2 formation, the activity order is CH/RhCu(1 1 1)≈CH_2/RhCu (1 1 1) > CH_3/RhCu(1 1 1) > RhCu(1 1 1).

3.1.4. CH_3 and methanol formation

CH_3 formation has only one route of CO + 3H → CHO + 2H → CH_2O + H → CH_3O → CH_3 + O. On the RhCu(1 1 1) and CH_x(x = 1–3)/RhCu(1 1 1) surfaces, as shown in Fig. 5, this route has the overall barriers of 275.3, 236.9, 273.2 and 226.7 kJ·mol^{-1}, which need to be endothermic by 179.4, 121.0, 170.7 and 125.0 kJ·mol^{-1}, respectively. Thus, the activity order of CH_3 formation is CH_3/RhCu(1 1 1) > CH/RhCu(1 1 1) > CH_2/RhCu(1 1 1)≈RhCu (1 1 1).

Methanol is generated by CH_3O or CH_2OH hydrogenation, which affects the productivity of CH_x(x = 1–3) intermediates and C_2 oxygenates. As displayed in Fig. 5(a)–(c), on the RhCu(1 1 1), CH/RhCu(1 1 1) and CH_2/RhCu(1 1 1) surfaces, the route of CO + 4H → CHO + 3H → CHOH + 2H → CH_2OH + H → CH_3OH dominantly contribute to methanol formation, this route has the overall barriers of 188.0, 136.2 and 174.8 kJ·mol^{-1}, which need to be endothermic by 116.0, 92.2 and 119.1 kJ·mol^{-1}, respectively. However, on CH_3/RhCu(1 1 1) surface (see Fig. 5(d)), CO + 4H → CHO + 3H → CH_2O + 2H → CH_3O + H → CH_3OH is the main route of methanol formation, which has the overall barrier of 159.4 kJ·mol^{-1}, and it needs to be endothermic by 59.4 kJ·mol^{-1}. Thus, the catalytic activity order of methanol formation is CH/RhCu(1 1 1) > CH_3/RhCu(1 1 1) > CH_2/RhCu(1 1 1) > RhCu(1 1 1).

Based on above results, it is concluded that in comparison with the clean RhCu(1 1 1) surface, the surface adsorbed CH_x(x = 1–3) intermediate acted as a co-adsorbed promoter not only promote the formation of CH_3 and methanol, but also alter the optimal route of methanol formation. Moreover, compared to CH_3 formation, methanol formation is more preferred in kinetics, which agree with the previous studies on the Cu-based or Rh-based catalysts [27,30,37,62,65].

3.1.5. The most favored CH_x monomer

Fig. 6(a) shows the overall barrier of the optimal CH, CH_2 and CH_3 formation route. On RhCu(1 1 1) surface, CH, CH_2 and CH_3 formation correspond to the overall barriers of 271.3, 224.6 and 275.3 kJ·mol^{-1}, respectively, indicating that the dominant CH_x monomer is CH_2 intermediate due to the lowest overall barrier of 224.6 kJ·mol^{-1}, our results are consistent with the reported results over RhCu(1 1 1) surface [11]. Similarly, on CH_x(x = 1–3)/RhCu (1 1 1) surface, the dominant CH_x monomer is also CH_2 intermediate. Namely, the dominant CH_x monomer is CH_2 over RhCu(1 1 1) and CH_x(x = 1–3)/RhCu(1 1 1) surfaces. More importantly, CH_x(x = 1–3)/RhCu(1 1 1) surface is more preferred for CH_2 formation in kinetics than the clean RhCu(1 1 1) surface. In addition, previous studies about syngas conversion also found that the dominant

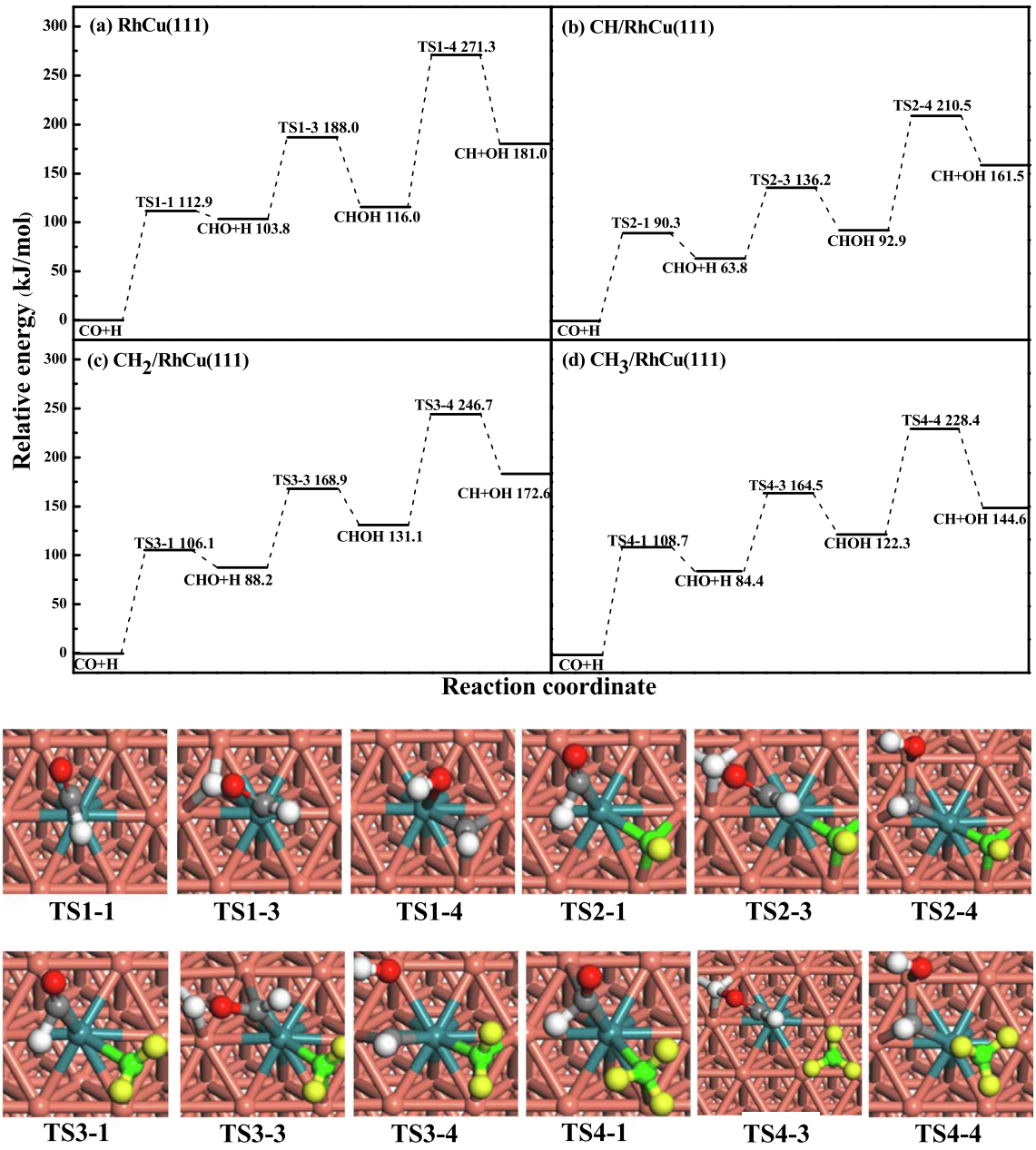

Fig. 3. The potential energy profiles for the most favorable route of CH formation with the transition states on the (a) RhCu(1 1 1), (b) CH/RhCu(1 1 1), (c) CH_2/RhCu(1 1 1), and (d) CH_3/RhCu(1 1 1). Orange, dark green, red balls represent Cu, Rh, O atoms, respectively. Gray and while balls are C and H atoms involving in the reaction, green and yellow balls are the C and H atoms of co-adsorbed promoter CH_x species that cannot participate into the reaction.

CH_x monomer is CH_2 intermediate on the Rh-based, Cu-based, and Co-based catalysts [34,35,37,65–69], for example, the isotope tracer by Jackson et al. [69] found that CH_2 is the key intermediate on Rh catalyst. Among all CH_x(x = 1–3) intermediates, Kapur et al. [35] theoretically proposed that CH_2 is the dominant monomer over the (1 1 1) and (2 1 1) surfaces of Rh catalyst, which is also supported over the Co(10–11) [67], Cu(1 1 1) [65], Cu(1 1 0) [37] and Fe-modified Cu(2 1 1) surfaces [34]. Meanwhile, as shown in Fig. 4, the optimal formation route of the dominant CH_2 monomer is different over four types of RhCu(1 1 1) surfaces.

Above results show that the presence of surface adsorbed CH_x(x = 1–3) intermediate as a co-adsorbed promoter not only promote the formation of the dominant CH_2 monomer, but also change the optimal formation route of CH_2. More importantly, CH_2 intermediate itself as the dominant CH_x(x = 1–3) monomer should be the dominant co-adsorbed promoter over RhCu(1 1 1) surface in syngas conversion.

3.2. The carbon chain formation of C_2 oxygenates

Previous studies show that when CH_x(x = 1–3) monomer is produced, four types of reactions related to CH_x(x = 1–3) may occur [5,19,27,30–34]: CH_x hydrogenation to methane, CH_x dissociation, CH_x reaction with CO/CHO to produce C_2 oxygenates, and CH_x coupling leading to C_2 hydrocarbons. The formation of hydrocarbons species (C_2 hydrocarbons and methane) decreases the selectivity of C_2 oxygenates [32,70,71]. Based on the dominant monomer CH_2 over the RhCu(1 1 1) and CH_x(x = 1–3)/RhCu(1 1 1) surfaces, in this study, all related reactions of CH_2 monomer, CH_2 dissociation to form CH, CH_2 successive hydrogenation to methane, CH_2

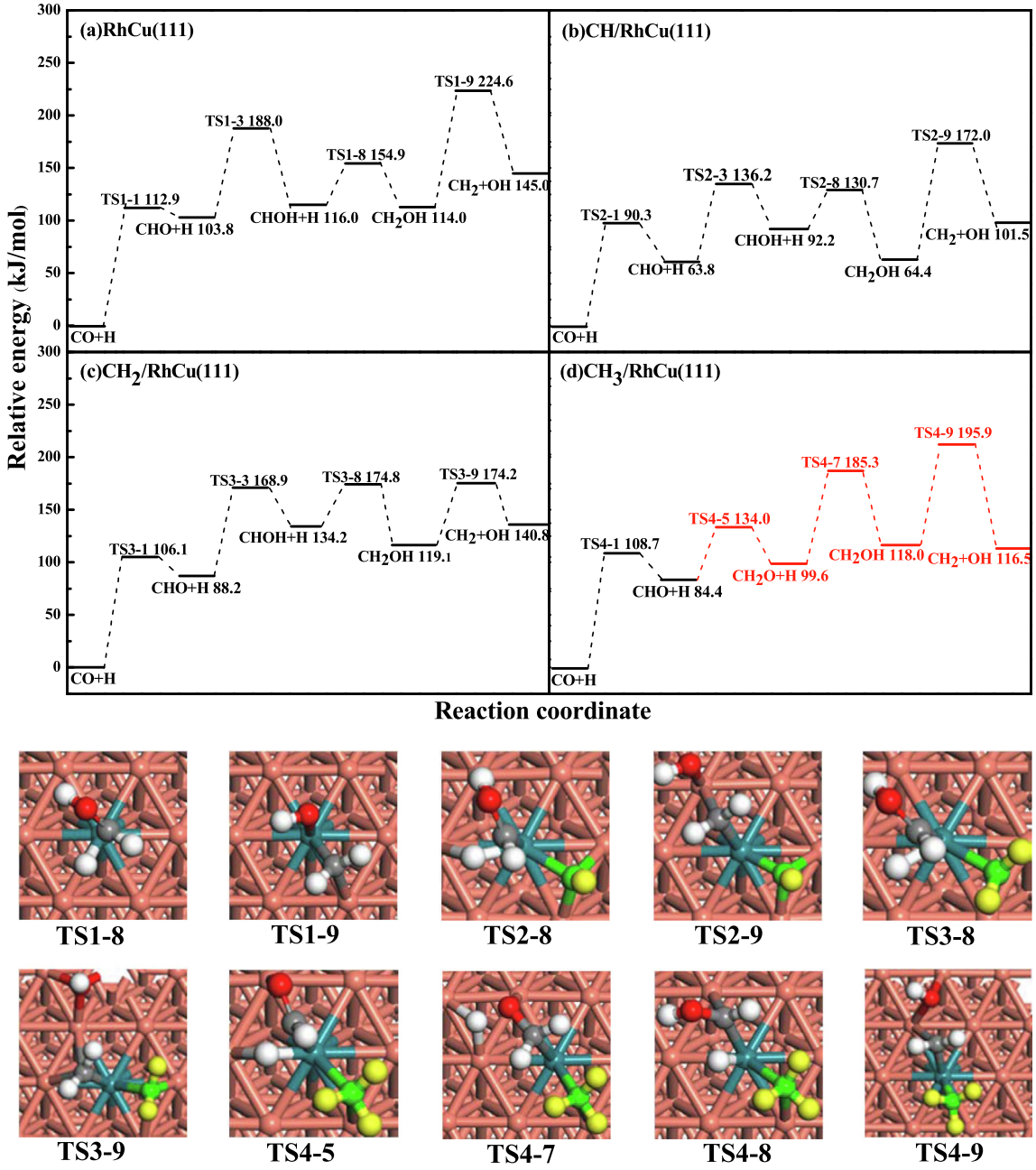

Fig. 4. The potential energy profiles for the most favorable route of CH_2 formation together with the transition states on (a) RhCu(1 1 1), (b) CH/RhCu(1 1 1), (c) CH_2/RhCu (1 1 1) and (d) CH_3/RhCu(1 1 1) surfaces.

self-coupling and CO/CHO reaction with CH_2 are examined, as listed in Table 1 (details in Fig. S8).

Fig. 7 presents the overall barrier of all reactions related to CH_2 monomer on the four surfaces. On RhCu(1 1 1), the formations of C_2 oxygenates and CH_4 is energetically competitive (31.9 *vs.* 35.4 kJ·mol^{-1}). However, on CH/RhCu(1 1 1), CH_2/RhCu(1 1 1) and CH_3/RhCu(1 1 1) surfaces, CHO reaction with CH_2 leading to C_2 oxygenates prefers to occur, which have the corresponding overall barriers of 34.6, 24.4 and 5.6 kJ·mol^{-1}, respectively; whereas the corresponding by-product mainly focus on the hydrocarbons CH_4, CH_4 and C_2H_4 corresponding to the overall barriers of 45.1, 46.0 and 36.0 kJ·mol^{-1}, respectively. Thus, CH_x(x = 1–3)/RhCu(1 1 1) exhibits better selectivity towards the formation of C_2 oxygenates compared to the clean RhCu(1 1 1) surface, indicating that the surface adsorbed CH_x(x = 1–3) intermediate acted as a co-adsorbed promoter over RhCu(1 1 1) surface promotes the formation of C_2 oxygenates in syngas conversion.

In addition, since the reactions related to CH_x species over the p (3 × 3) CH_x(x = 1–3)/RhCu(1 1 1) surfaces employed in this study have three species, the lateral interaction may affect the barrier for the reactions related to CH_x species. Meanwhile, our results show that CH_2/RhCu(1 1 1) surface significantly promote CH_2 formation compared to RhCu(1 1 1), CH/RhCu(1 1 1) and CH_3/RhCu (1 1 1) surfaces. As a result, the reactions related to CH_2 species over the p(4 × 4) CH_2/RhCu(1 1 1) surface are considered, moreover, the formation of CH_2CHO and major by-products (CH_4 and C_2H_4) over the p(4 × 4) CH_x(x = 1,3)/RhCu(1 1 1) surfaces are also examined (see details in the Part 5 of Supplementary Material). Our results show that the supercell size of CH_x(x = 1–3)/RhCu (1 1 1) surface can affect the values of the reaction barrier to a

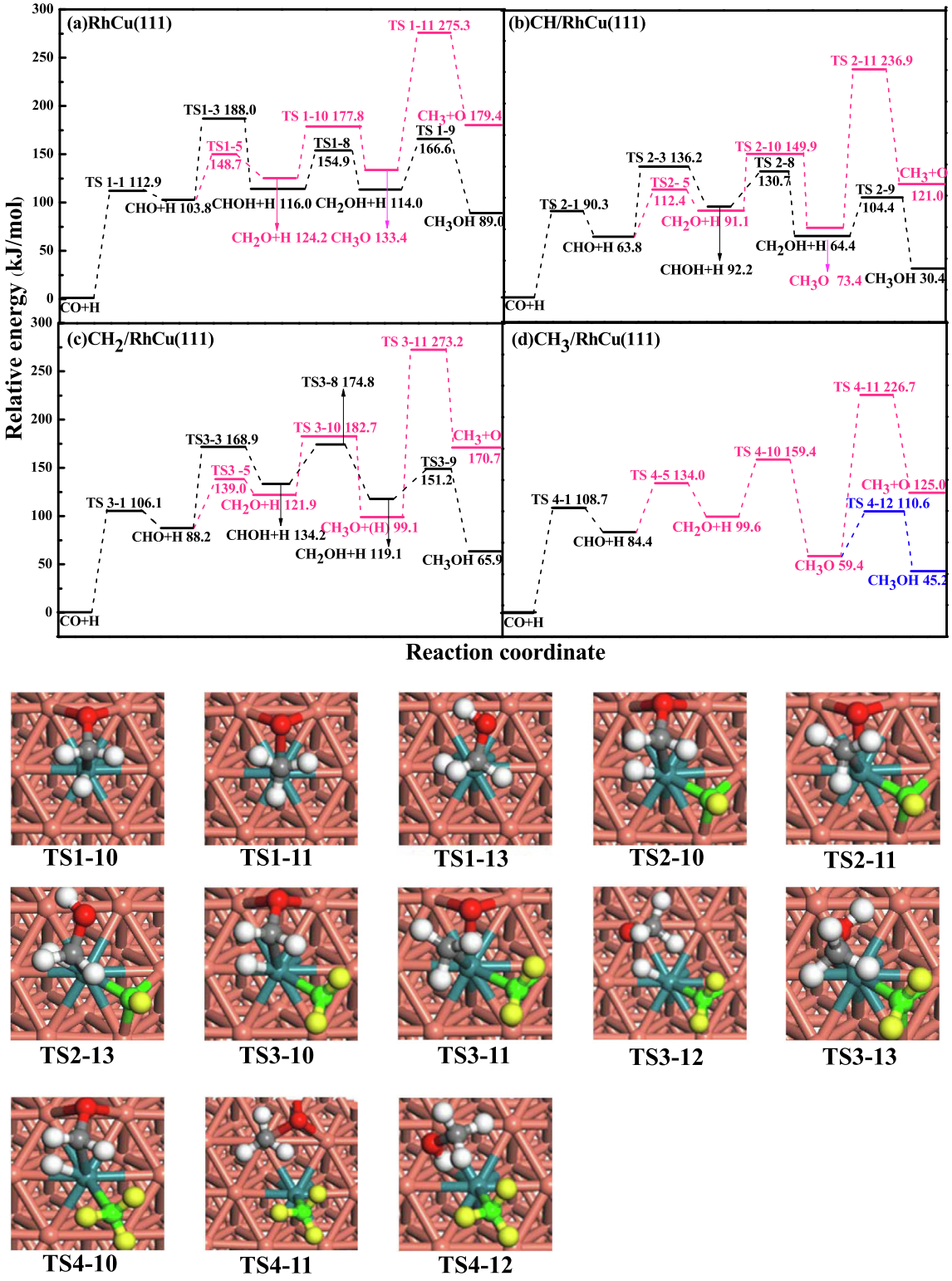

Fig. 5. The potential energy profiles for the most favorable route of CH_3 formation together with the transition states on (a) RhCu(1 1 1), (b) CH/RhCu(1 1 1), (c) CH_2/RhCu (1 1 1) and (d) CH_3/RhCu(1 1 1) surfaces.

small extent, however, C_2 oxygenates CH_2CHO is still the main product over the $p(4 \times 4)$ $CH_x(x = 1–3)$/RhCu(1 1 1) surfaces, suggesting that the results obtained over the $p(4 \times 4)$ $CH_x(x = 1–3)$/RhCu (1 1 1) surfaces agree with that obtained over the $p(3 \times 3)$ $CH_x(x = 1–3)$/RhCu(1 1 1) surfaces, namely, the $p(3 \times 3)$ $CH_x(x = 1–3)$/RhCu(1 1 1) surfaces employed in this study can well qualitatively reflect the new role of surface adsorbed $CH_x(x = 1–3)$ intermediates as a co-adsorbed promoter in self-promoting syngas conversion to form CH_x intermediates and C_2 oxygenates on the Rh-doped Cu catalyst.

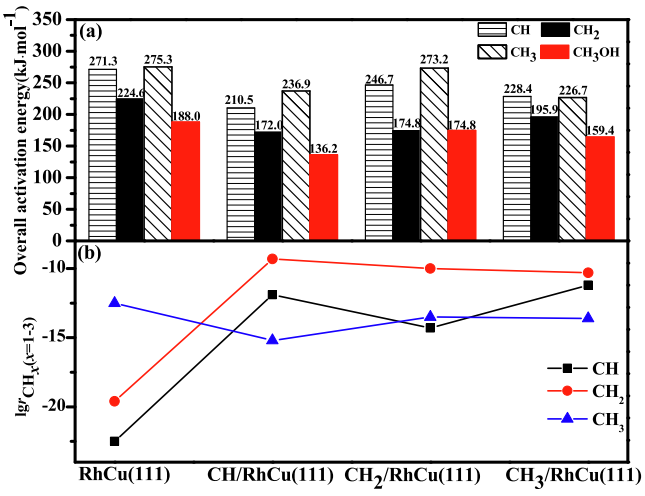

Fig. 6. (a) The overall barrier for the most favorable formation routes of CH_x(x = 1–3) and CH_3OH with respect to CO + H species, (b) the reaction rates of CH_x(x = 1–3) formation over the RhCu(1 1 1) and CH_x(x = 1–3)/RhCu(1 1 1) surfaces at 523 K.

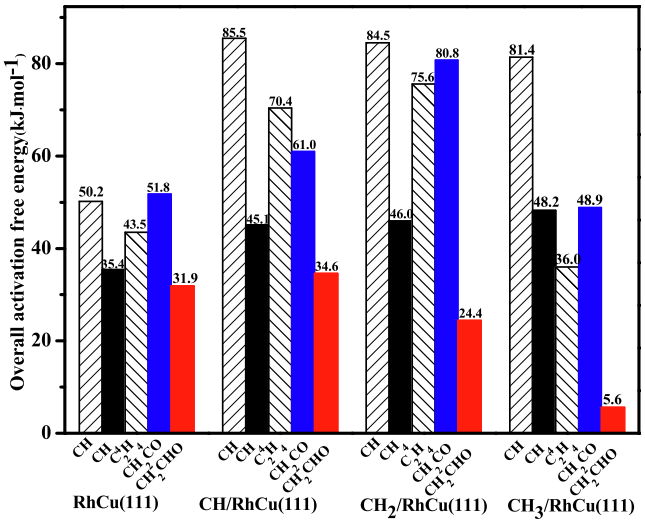

Fig. 7. The overall barriers for the reactions related to CH_2 species on RhCu(1 1 1) and CH_x(x = 1–3)/RhCu(1 1 1) surfaces at 523 K.

3.3. General discussions

3.3.1. The role of adsorbed CH_x(x = 1–3) intermediates in the CH_x formation

Based on the above analysis, as shown in Fig. 6(a), the overall formation barrier of CH_x(x = 1–3) intermediates over RhCu(1 1 1) surface is higher than that over CH_x(x = 1–3)/RhCu(1 1 1) surface, indicating that the surface adsorbed CH_x(x = 1–3) intermediate acted as a co-adsorbed promoter in syngas conversion over RhCu (1 1 1) surface enhances the catalytic activity of CH_x(x = 1–3) itself formation. Especially, for the dominant CH_2 monomer, the activity order of CH_2 formation is CH/RhCu(1 1 1) ≈ CH_2/RhCu(1 1 1) > CH_3/RhCu(1 1 1) > RhCu(1 1 1). Further, taking the coverage of surface intermediates in the process of CO activation to form CH_x intermediates into consideration, the reaction rates of CO activation to form CH_x species based on a microkinetic modeling using the data presented in Table 1 (see details in the Part 7 of Supplementary Material) are calculated, the microkinetic model [30,67,72,73] has been widely applied in CO activation to form CH_x species with the aim of estimating the reaction rate of CH_x(x = 1–3) under the typical experimental conditions (P_{CO} = 4 atm, P_{H2} = 8 atm; T = 523 K). As shown in Fig. 6(b), the results obtained by Microkinetic modeling show that the formation rate for CO activation to form CH_2 intermediate is much higher than those of CH and CH_3 intermediates over the CH_x(x = 1–3)/RhCu(1 1 1) surfaces, as well as those of CH_x(x = 1–3) intermediates over the pure RhCu(1 1 1) surface; as a result, compared to the pure RhCu(1 1 1) surface, the surface adsorbed CH_x(x = 1–3) species acted as a co-adsorbed promoter over RhCu(1 1 1) surface exhibit the highest catalytic activity toward CO activation to form the dominant monomer CH_2 among all CH_x(x = 1–3) intermediates, which agree with our above results obtained by DFT calculations (the activation barrier), as shown in Fig. 6(a). However, it is noted that our DFT results suggest that CH_2 monomer is preferentially formed on the pure RhCu (1 1 1) surface, which is not in agreement with the microkinetic modeling that CH_3 monomer is preferentially formed; this phenomenon can be attributed to the formation rate of products not only rely on the rate constant (determined by the activation barrier), but also depend on the coverage of key intermediates involving CO activation to form CH_x(x = 1–3).

On the other hand, in syngas conversion on Cu-based catalysts, CO successive hydrogenation can also produce methanol [27,37,38,65,69], by decreasing the formation barrier of CH_x(x = 1–3) and/or increasing that of methanol, in this way, methanol formation can be suppressed, and more CH_x intermediates will be formed. The results show that methanol prefers to be formed in kinetics rather than the CH_x(x = 1–3) intermediates on the RhCu (1 1 1) and CH_x(x = 1,3)/RhCu(1 1 1) surfaces, which exhibits better selectivity towards methanol formation. However, the dominant monomer CH_2 formation kinetically competes with methanol formation on CH_2/RhCu(1 1 1) due to the close overall barriers of 174.8 and 174.8 kJ·mol^{-1}, the formed methanol quickly desorbs from the surface, namely, CH_2/RhCu(1 1 1) surface significantly improves the selectivity towards CH_2 formation compared to the clean RhCu(1 1 1), CH/RhCu(1 1 1) and CH_3/RhCu(1 1 1) surfaces.

Previous researches about syngas conversion over the (1 1 1) [30,35] and (2 1 1) [35] surfaces of Rh catalyst, as well as the (1 0 0) [38], (1 1 0) [37], (1 1 1) [65] and (2 1 1) [27] surfaces of Cu catalyst do not considered CH_x(x = 1–3) intermediate itself as the co-adsorbed promoter, which showed that methanol formation was more preferred in kinetics over CH_x(x = 1–3) formation. However, in this study, the surface adsorbed CH_x(x = 1–3) intermediate itself is considered to act as a co-adsorbed promoter for the formation of CH_x intermediates over RhCu(1 1 1) surface, it presents a positive effect for the catalytic activity enhancement of CO activation to form CH_x(x = 1–3) intermediate, especially, the dominant CH_2 intermediate acted as a co-adsorbed promoter exhibits excellent catalytic activity and selectivity towards itself formation, and effectively inhibit methanol formation, and therefore the abundant CH_2 sources are provided for the subsequent reactions of C_2 oxygenates formation.

3.3.2. The role of adsorbed CH_x(x = 1–3) intermediate in the C_2 oxygenates formation

Under the conditions that the surface adsorbed CH_x intermediate itself is not considered as a co-adsorbed promoter, previous studies [19] found that the reactions related to CH_x intermediates on the (1 1 1) and (5 5 3) surfaces of Rh catalyst mainly contribute to CH_4 formation instead of C_2 oxygenates. Moreover, Choi and Liu [30], Kapur et al. [35], Yang et al. [61] also confirmed that CH_4 or C_2 hydrocarbons are the main products in syngas conversion on the (1 1 1) and (2 1 1) surfaces of Rh catalyst. Further, CH_4 formation is energetically competitive with C_2 oxygenates on the Rh-doped Cu(1 1 1) [19] and the Rh-doped Cu(2 1 1) [71] surfaces.

As presented in Fig. 7, on the clean RhCu(1 1 1) surface, C_2 oxygenates and methane are the dominant products due to the close overall barriers, which agree with that on the RhCu(1 1 1) and RhCu(2 1 1) surfaces [19,71]. However, on $CH_x(x = 1–3)$/RhCu (1 1 1) surface, C_2 oxygenates CH_2CHO becomes to be the main product, indicating that the surface adsorbed $CH_x(x = 1–3)$ intermediate itself acted as a co-adsorbed promoter over RhCu(1 1 1) surface exhibits better selectivity towards C_2 oxygenates; meanwhile, the selectivity between CH_2CHO and major by-products (CH_4 and C_2H_4) is quantitatively analyzed using the barrier difference between CH_2CHO and major by-products as a descriptor. The larger barrier difference means that CH_2CHO has higher selectivity and the by-product has lower selectivity. Our results show that the barrier differences on the RhCu(1 1 1) and $CH_x(x = 1–3)$/RhCu (1 1 1) surfaces correspond to the values of 3.5, 10.5, 21.6 and 30.4 kJ·mol^{-1}, respectively. Thus, CH_2CHO selectivity follows the order of CH_3/RhCu(1 1 1) > CH_2/RhCu(1 1 1) > CH/RhCu(1 1 1) > RhCu(1 1 1).

Among the four RhCu(1 1 1) surfaces studied, compared to the clean RhCu(1 1 1) surface (31.9 kJ·mol^{-1}), CH_2/RhCu(1 1 1) or CH_3/RhCu(1 1 1) surface with the surface adsorbed CH_2 or CH_3 intermediates acted as a co-adsorbed promoter exhibit a highly catalytic activity for CH_2CHO formation due to the small barriers (24.4 or 5.6 kJ·mol^{-1}), whereas CH intermediate has little effect on the catalytic activity (34.6 kJ·mol^{-1}). The activity of CH_2CHO formation follows the order of CH_3/RhCu(1 1 1) > CH_2/RhCu (1 1 1) > RhCu(1 1 1) > CH/RhCu(1 1 1).

On the basis of above analysis, the surface adsorbed CH_2 or CH_3 intermediates acted as a co-adsorbed promoter over RhCu(1 1 1) surface significantly enhances the catalytic activity and selectivity of C_2 oxygenates. Although CH_3 intermediate is more preferred over CH_2 intermediate, CH_2 intermediate itself as the dominant monomer should played a dominant role in promoting the formation of C_2 oxygenates.

In addition, as mentioned above, CH_2/RhCu(1 1 1) surface significantly promote CH_2 formation compared to RhCu(1 1 1), CH/RhCu(1 1 1) and CH_3/RhCu(1 1 1) surfaces, moreover, CH_2 intermediate itself as the dominant monomer played a dominant role in promoting the formation of C_2 oxygenates by CHO insertion into CH_2. However, for the reactions of CHO insertion into CH_2 over CH_2/RhCu(1 1 1) surface, it is noted that surface adsorbed CH_2 intermediates may react with the co-adsorbed promoter CH_2, correspondingly, CHO species will act as the co-adsorbed promoter over RhCu(1 1 1) surface, which is denoted as CHO/RhCu(1 1 1) surface, as shown in Fig. S13, the results show that the reactions of CH_2 coupling with CH_2 in the presence of CHO species over CHO/RhCu(1 1 1) surface is still difficult in kinetics than the reaction of CHO insertion into CH_2 in the presence of CH_2 species over CH_2/RhCu(1 1 1) surface (71.8 *vs.* 24.4 kJ/mol). On the other hand, in the formation process of the favored CH_2 monomer via CH_2O and CH_2OH dissociation, OH species can be formed to affect the reactions of syngas conversion, thus, the effect of OH species acted as a co-adsorbed promoter on the key elementary reactions in syngas conversion to form C_2 oxygenates including CO + H → CHO for CO activation, $CH_2OH \rightarrow CH_2 + OH$ for CH_2 formation, CHO + $CH_2 \rightarrow CH_2CHO$ for C_2 oxygenates formation, were further investigated. As shown in Fig. S14, compared to RhCu(1 1 1) surface, OH-species over RhCu(1 1 1) surface denoted as OH/RhCu (1 1 1) surface with OH-species acted as a co-adsorbed promoter can promote these three elementary reactions. However, compared to the $CH_x(x = 1–3)$/RhCu(1 1 1) surface, the effect of OH/RhCu (1 1 1) surface on these elementary reactions is weaker, namely, the promotion effect of OH species acted as a co-adsorbed promoter is weaker than that of CH_x species acted as a co-adsorbed promoter over the RhCu(1 1 1) surface.

3.3.3. The analysis of electronic properties

Based on above results, once the dominant monomer CH_2 intermediate is produced over $CH_x(x = 1–3)$/RhCu(1 1 1) surface, C_2 oxygenates preferred to be formed with high selectivity. Thus, CO activation and conversion to form the dominant CH_2 intermediate becomes a crucial step in syngas conversion to C_2 oxygenates. Aiming at further determining the microscopic reason why the surface adsorbed $CH_x(x = 1–3)$ intermediates as a co-adsorbed promoter over RhCu(1 1 1) surface play a new and key role in CO activation to form the dominant monomer CH_2, the analysis of electronic properties is carried out to obtain the correlation between electronic properties and catalytic performance.

As shown in Fig. 8, the differential charge density of RhCu(1 1 1) and $CH_x(x = 1–3)$/RhCu(1 1 1) surfaces showed that Cu loses electrons and Rh accepts electrons, which is in accordance with the results obtained by Rodriguez et al. [24]. Meanwhile, the Bader charge is calculated to quantitatively analyze the number of electrons accepted by Rh atom, the Bader charge of Rh atom are

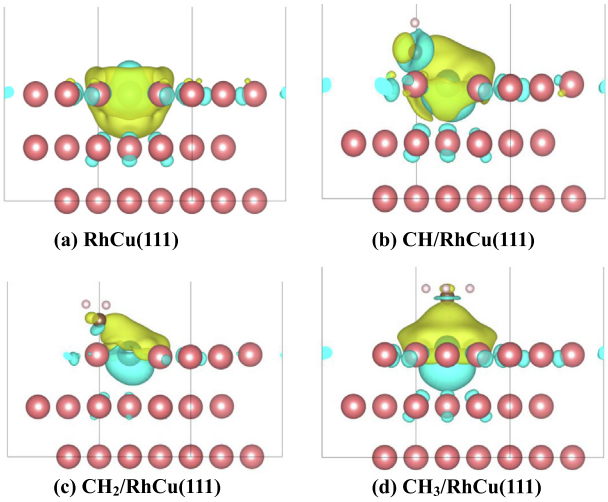

Fig. 8. Differential charge density of Rh atom and its surrounding Cu atoms on the RhCu(1 1 1) and $CH_x(x = 1–3)$/RhCu(1 1 1) surfaces. The blue and yellow shaded regions represent the charge loss and charge gain, respectively. The values of absolute isosurface is 0.003 e·Å^{-3}.

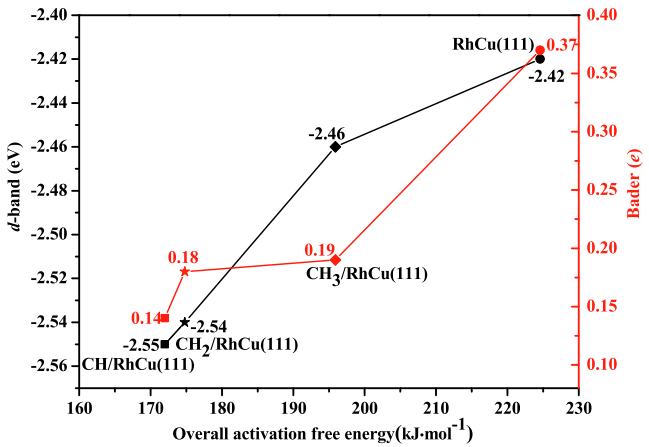

Fig. 9. The relationship between the activity of CO activation to $CH_x(x = 1–3)$ and the surface *d*-band center or the Bader charge of Rh atom over the RhCu(1 1 1) and $CH_x(x = 1–3)$/RhCu(1 1 1) surfaces. The *d*-band center corresponds to the Rh atoms and its adjacent surface and subsurface Cu atoms over the RhCu(1 1 1) and $CH_x(x = 1–3)$/RhCu(1 1 1) surfaces.

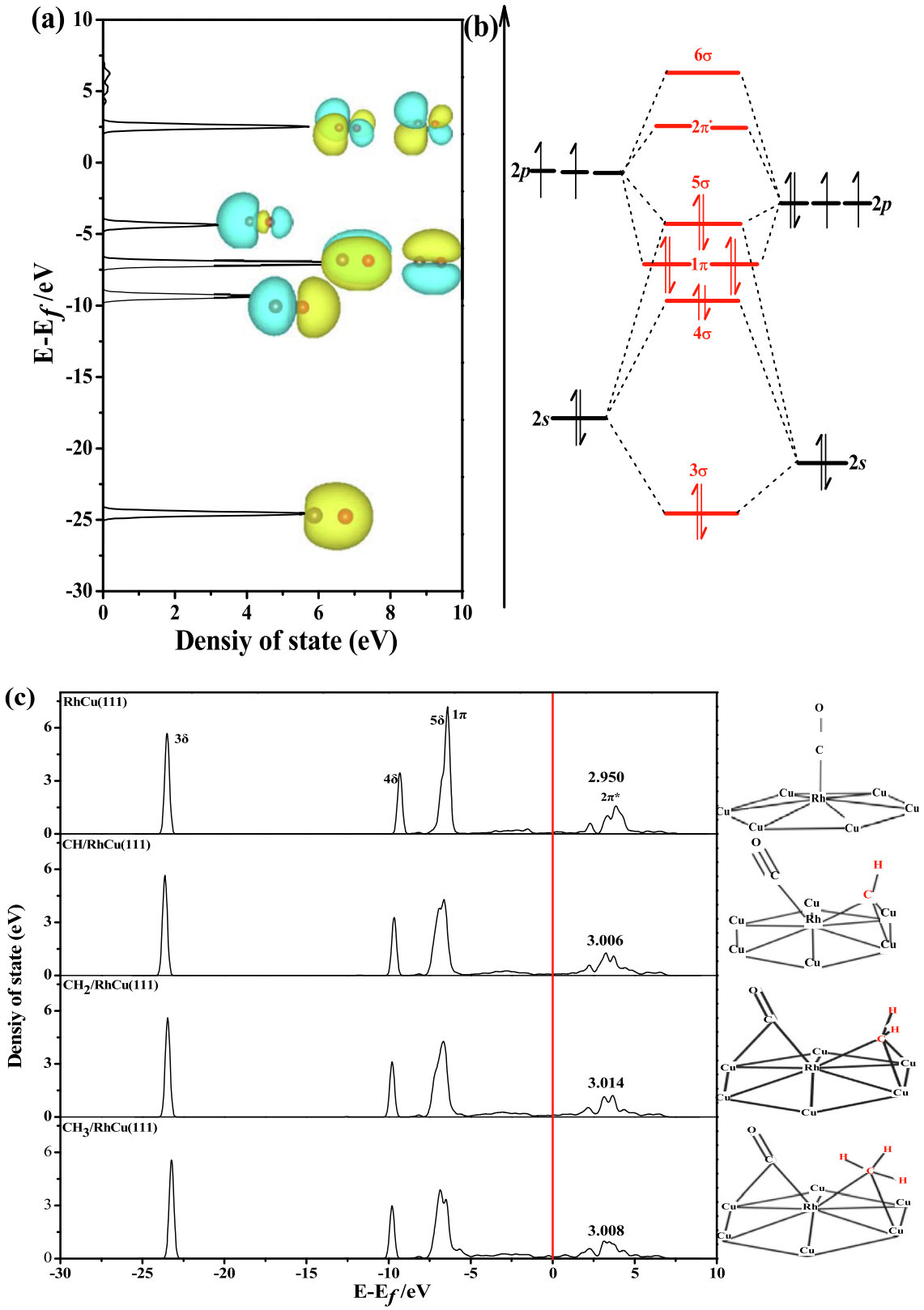

Fig. 10. (a) Gas phase CO DOS curves with respective electron isodensity surfaces representing each molecule orbital (MO), (b) MO, and (c) DOS of CO adsorbed at the most stable sites of the RhCu(1 1 1), CH/RhCu(1 1 1), CH_2/RhCu(1 1 1) and CH_3/RhCu(1 1 1) surfaces.

−0.37, −0.14, −0.18 and −0.19 *e* on the RhCu(1 1 1), CH/RhCu (1 1 1), CH_2/RhCu(1 1 1) and CH_3/RhCu(1 1 1) surfaces, respectively; Namely, in comparison with the clean RhCu(1 1 1) surface, CH_x(x = 1–3)/RhCu(1 1 1) surface with the surface adsorbed CH_x(x = 1–3) intermediates decreases the number of electrons accepted by Rh atom, which weakens the adsorption ability of key CH_xO(x = 0–3) and CH_xOH(x = 1,2) intermediates. On the other hand, the *d*-electrons and/or empty *d*-orbitals of transition metals

[74–77] are closely related to their catalytic activity, and the location of *d*-band center determines the adsorption strength of adsorbed species. As shown in the black line of Fig. 9, the deviation degree of *d*-band center from the Fermi level are −2.42, −2.55, −2.54 and −2.46 eV on the RhCu(1 1 1) and CH_x(x = 1–3)/RhCu (1 1 1) surfaces, respectively, suggesting that the presence of surface adsorbed CH_x(x = 1–3) intermediates makes the *d*-band center far from the Fermi level compared to the clean RhCu (1 1 1) surface, which also weakens the adsorption ability of key CH_xO(x = 1–3) and CH_xOH(x = 1,2) intermediates.

As mentioned above, the surface adsorbed CH_x(x = 1–3) intermediates decreases the adsorption ability of CH_xO(x = 1–3) and CH_xOH(x = 1,2) intermediates, which originate from the lateral interaction between the key intermediates and the co-adsorbed CH_x intermediate as a promoter. As a result, the decreasing of adsorption ability promotes the migration of these key intermediates towards their more favorable active sites [64], which is more favorable for the C—O bond cleavage of these key intermediates leading to the catalytic activity enhancement of CH_x(x = 1–3) intermediates formation. The results obtained by the analysis of electronic properties agree with our kinetics results. In addition, Zha et al. [48] showed that compared to the presence of H atoms, the presence of OH intermediate is favorable for decreasing the adsorption energy of reaction intermediates in the process of CH_x(x = 1–3) formation, and improves their migration ability among the surface active sites, thereby the presence of OH species promotes CO activation to form CH_x intermediates.

In order to further verify that the adsorption site that is after the migration of surface species is more favorable for CO activation to form CH_x intermediates, the projected density of states (*p*DOS) onto the C—O bond of CO were calculated to probe into the role of surface adsorbed CH_x(x = 1–3) intermediates. The primary shifting of $2\pi^*$ bands is due to the electron donation from the *d* orbital of metal catalyst to the $2\pi^*$ orbital of CO [78]. We firstly consider the gas phase CO molecule, the C/O *p*DOS together with the electron density isosurfaces of the MOs and CO molecular orbital diagram are depicted in Fig. 10(a) and (b), respectively. The *p*DOS results of adsorbed CO (see Fig. 10(c)) show that the electron population of $2\pi^*$ anti-bonding orbital for CO adsorbed on the CH/RhCu (1 1 1), CH_2/RhCu(1 1 1) and CH_3/RhCu(1 1 1) surfaces are 3.006, 3.014, and 3.008 *e*, respectively, which were higher than that (2.950 *e*) on the clean RhCu(1 1 1) surface. In other words, the more electron transfer from the *d*-orbital of metal catalyst to the adsorbed CO anti-bonding orbital means the more significant weakening of the C—O bond [78,79]. Therefore, the adsorption site after CO migration is more favorable for the C—O bond activation of CO, which further confirms our kinetics results.

In general, compared to the traditional understandings about the role of CH_x species as the reactive intermediate in syngas conversion to C_2 oxygenates, a new fundamental mechanism about the role of surface adsorbed CH_x intermediates is proposed in this study, that is, the surface adsorbed CH_x intermediate itself can act as a co-adsorbed promoter to self-promote CO activation and conversion to C_2 oxygenates with high catalytic activity and selectivity. This so-called CH_x self-promoting syngas conversion open a new mechanism that is likely general and involved in the reactions related to the formation of CH_x(x = 1–3) intermediates.

4. Conclusions

This study employed density functional theory calculations to reveal the new role of surface adsorbed CH_x(x = 1–3) intermediates as a co-adsorbed promoter in self-promoting syngas conversion to form the CH_x intermediates and C_2 oxygenates over the Rh-doped Cu catalyst. The Rh-doped Cu catalyst is modeled using the clean RhCu(1 1 1) and CH_x(x = 1–3)/RhCu(1 1 1) surfaces. The results show that methanol formation is more favorable than CH_x(x = 1–3) intermediates on the clean RhCu(1 1 1) surface, however, the surface adsorbed CH_x(x = 1–3) intermediates as a co-adsorbed promoter over RhCu(1 1 1) surface not only significantly promote the formation of the dominant monomer CH_2, but also inhibit methanol formation. Especially, the dominant monomer CH_2 acted as a co-adsorbed promoter exhibits higher catalytic activity and selectivity towards its self-formation. Further, starting from the dominant monomer CH_2, CH_4 formation on the clean RhCu(1 1 1) surface is energetically competitive with C_2 oxygenates CH_2CHO; however, CH_x(x = 1–3)/RhCu(1 1 1) surface exhibits higher selectivity towards CH_2CHO by CHO reaction with CH_2 instead of the hydrocarbons, especially, CH_2/RhCu(1 1 1) and CH_3/RhCu(1 1 1) surfaces significantly enhance the activity and selectivity of C_2 oxygenates in comparison with the clean RhCu(1 1 1) and CH_3/RhCu (1 1 1) surfaces. Taking the dominant monomer CH_2 and the C—C chain of C_2 oxygenates into account, compared to the clean RhCu (1 1 1) surface, the surface adsorbed CH_2 intermediate as a co-adsorbed promoter over RhCu(1 1 1) surface played a fundamental role in self-promoting syngas conversion to form C_2 oxygenates, which significantly improved the activity and selectivity of syngas conversion to form C_2 oxygenates, and inhibit the formation of methanol and hydrocarbons.

The analysis of electronic properties including the differential charge density, the Bader charge and the *d*-band center give out the microscopic reason why the surface adsorbed CH_x(x = 1–3) intermediates as a co-adsorbed promoter over RhCu(1 1 1) surface play a key role in CO activation to form CH_x intermediate. The correlation between electronic properties and catalytic performance is obtained. A new mechanism for the new role of surface adsorbed CH_x(x = 1–3) intermediates has been proposed, that is: the surface adsorbed CH_x(x = 1–3) intermediate itself can acted as a co-adsorbed promoter on RhCu(1 1 1) surface to promote the migration of key intermediates CH_xO(x = 1–3) or CH_xOH(x = 1,2) towards their more favorable active sites, which is more favorable for the C—O bond cleavage of these key intermediates; Thus, the catalytic activity of CH_x(x = 1–3) formation in CO activation is enhanced.

Acknowledgment

This work is financially supported by the Key projects of National Natural Science Foundation of China (No. 21736007), the National Natural Science Foundation of China (No. 21776193, 21476155), the China Scholarship Council (201606935026) and the Top Young Innovative Talents of Shanxi.

Appendix A. Supplementary material

The computational details and supplementary date, including the methods for calculating the relevant energy, the adsorption and co-adsorption behaviors of key intermediates, the reactions of CO activation to form CH_x intermediates, the reactions related to CH_2 species, the reactions related to CH_x species over the *p* (4 × 4) surfaces, Microkinetic modeling and the *d*-band analysis are all described in detail. Supplementary data to this article can be found online at https://doi.org/10.1016/j.jcat.2019.07.019.

References

[1] J.P. Hindermann, G.J. Hutchings, A. Kiennemann, Catal. Rev.: Sci. Eng. 35 (1993) 1–127.
[2] V. Subramani, S.K. Gangwal, Energy Fuels 22 (2008) 814–839.
[3] S.C. Chuang, J.G. Goodwin, J.R.I. Wender, J. Catal. 95 (1995) 435–446.
[4] X.L. Pan, Z.L. Fan, W. Chen, Y.J. Ding, H.Y. Luo, X.H. Bao, Nat. Mater. 6 (2007) 507–511.
[5] S.S.C. Chuang, R.W. Stevens Jr., R. Khatri, Top. Catal. 32 (2005) 225–232.

[6] D. Ding, J. Yu, Q. Guo, X. Guo, H. Mao, D. Mao, Catal. Lett. 148 (2018) 1–8.
[7] N.D. Subramanian, J. Gao, X.H. Mo, J.G. Goodwin Jr., W. Torres, J.J. Spivey, J. Catal. 272 (2010) 204–209.
[8] H. Ngo, Y.Y. Liu, K. Murata, React. Kinet. Mech. Cat. 102 (2011) 425–435.
[9] L.P. Han, D.S. Mao, J. Yu, Q.S. Guo, G.Z. Lu, Catal. Commun. 23 (2012) 20–24.
[10] S. Zaman, K.J. Smith, Catal. Rev. 54 (2012) 41–132.
[11] M. Konarova, F.Q. Tang, J.L. Chen, G. Wang, V. Rudolph, J. Beltramini, ChemCatChem 6 (2014) 2394–2402.
[12] Y.Z. Yang, X.Z. Qi, X.X. Wang, D. Lv, F. Yu, L.S. Zhong, H. Wang, Y.H. Sun, Catal. Today 270 (2016) 101–107.
[13] M. Ao, G.H. Phama, V. Sage, V. Pareek, Fuel 206 (2017) 390–400.
[14] M. Ding, J. Tu, M. Qiu, T. Wang, L. Ma, Y. Li, Appl. Energy 138 (2015) 584–589.
[15] X.M. Yang, Y. Wei, Y.L. Su, L.P. Zhou, Fuel Process. Technol. 91 (2010) 1168–1173.
[16] K.J. Smith, R.B. Anderson, Can. J. Chem. Eng. 61 (1983) 40–45.
[17] M. Gupta, M.L. Smith, J.J. Spivey, ACS Catal. 1 (2011) 641–656.
[18] S. Jie, Q.X. Cai, Y. Wan, S.L. Wan, L. Wang, J.D. Lin, D.H. Mei, Y. Wang, ACS Catal. 6 (2016) 5771–5785.
[19] Y.H. Zhao, M.M. Yang, D.P. Sun, H.Y. Su, K.J. Sun, X.F. Ma, X.H. Bao, W.X. Li, J. Phys. Chem. C 115 (2011) 18247–18256.
[20] T. Komatsu, H. Kobayashi, K. Kusada, Y. Kubota, M. Takata, T. Yamamoto, S. Matsumura, K. Sato, K. Nagaoka, H. Kitagawa, Chem. – Eur. J. 23 (2016) 57–60.
[21] T.B. Massalsiki, H. Okamoto, P.R. Subramanian, L. Kacprezak, Binary Alloy Phase Diagrams, second ed., ASM: Materials Parks, OH, 1992.
[22] L. Irons, S. Mini, B.E. Brower, Mater. Sci. Eng. 98 (1988) 309–312.
[23] S.C. Chou, C.T. Yeh, T.H. Chang, J. Phys. Chem. B 101 (1997) 5828–5833.
[24] J.A. Rodriguez, R.A. Campbell, D.W. Goodman, J. Phys. Chem. 94 (1990) 6936–6939.
[25] S. Gonzalez, C. Sousa, F. Illas, Surf. Sci. 531 (2003) 39–52.
[26] N. Lopez, J.K. Norskov, Surf. Sci. 477 (2001) 59–75.
[27] R.G. Zhang, G.R. Wang, B.J. Wang, J. Catal. 305 (2013) 238–255.
[28] F. Fischer, H. Tropsch, Brennst. Chem. 7 (1926) 97–116.
[29] H. Pichler, H. Schulz, Chem. Ing. Tech. 42 (1970) 1162–1174.
[30] Y. Choi, P. Liu, J. Am. Chem. Soc. 131 (2009) 13054–13061.
[31] M. Ichikawa, T. Fukushima, J. Chem. Soc., Chem. Commun. 1 (1985) 321–323.
[32] Y.H. Zhao, K.J. Sun, X.F. Ma, J.X. Liu, D.P. Sun, H.Y. Su, W.X. Li, Angew. Chem. Int. Ed. 50 (2011) 5335–5338.
[33] R.G. Zhang, M. Peng, B.J. Wang, Catal. Sci. Technol. 7 (2017) 1073–1085.
[34] L.X. Ling, Q. Wang, R.G. Zhang, D.B. Li, B.J. Wang, Phys. Chem. Chem. Phys. 19 (2017) 30883–30894.
[35] N. Kapur, J.H. Yun, B. Shan, J.B. Nicholas, K. Cho, J. Phys. Chem. C 114 (2010) 10171–10182.
[36] G.X. Wen, Q. Wang, R.G. Zhang, D.B. Li, B.J. Wang, Phys. Chem. Chem. Phys. 18 (2016) 27272–27283.
[37] R.G. Zhang, X.C. Sun, B.J. Wang, J. Phys. Chem. C 117 (2013) 6594–6606.
[38] H.Y. Zheng, R.G. Zhang, Z. Li, B.J. Wang, J. Mol. Catal. A: Chem. 404–405 (2015) 115–130.
[39] S.Y. Chin, C.T. Williams, M.D. Amiridis, J. Phys. Chem. B 110 (2006) 871–882.
[40] S. Krishnamoorthy, M. Tu, M.P. Ojeda, D. Pinna, E. Iglesia, J. Catal. 211 (2002) 422–433.
[41] S. Loegdberg, M. Boutonnet, J.C. Walmsley, S. Jaeras, A. Holmen, E.A. Blekkan, Appl. Catal. A: Gen. 393 (2011) 109–121.
[42] W.P. Ma, G. Jacobs, D.E. Sparks, R.L. Spicer, B.H. Davis, J.L.S. Klettlinger, C.H. Yen, Catal. Today 228 (2014) 158–166.
[43] A.K. Dalai, T.K. Das, K.V. Chaudhari, G. Jacobs, B.H. Davis, Appl. Catal. A: Gen. 289 (2005) 135–142.
[44] E. Jiménez-Barrera, P. Bazin, C. Lopez-Cartesc, F. Romero-Sarriaa, M. Daturi, J.A. Odriozola, Appl. Catal. B: Environ. 237 (2018) 986–995.
[45] S. Storsæter, Ø. Borg, E.A. Blekkan, A. Holmen, J. Catal. 231 (2005) 405–419.
[46] J. Schweicher, A. Bundhoo, N. Kruse, J. Am. Chem. Soc. 134 (2012) 16135–16138.
[47] G.K.K. Gunasooriya, A.P. van Bavel, H.P. Kuipers, M. Saeys, ACS Catal. 6 (2016) 3660–3664.
[48] H. Zha, X.Q. Dong, Y.Z. Yu, M.H. Zhang, Surf. Sci. 669 (2018) 114–120.
[49] J. Furthmüller, J. Hafner, G. Kresse, Phys. Rev. B: Condens. Matter Mater. Phys. 54 (1996) 11169–11186.
[50] G. Kresse, J. Furthmüller, Comput. Mater. Sci. 6 (1996) 15–50.
[51] J.P. Perdew, K. Burke, M. Ernzerhof, Phys. Rev. Lett. 77 (1996) 3865–3868.
[52] G. Henkelman, B.P. Uberuaga, H.A. Jónsson, J. Chem. Phys. 113 (2000) 9901–9904.
[53] G. Henkelman, H.A. Jónsson, J. Chem. Phys. 111 (1999) 7010–7022.
[54] H. Graeme, J. Hannes, J. Chem. Phys. 111 (1999) 7010–7022.
[55] R.A. Olsen, G.J. Kroes, G. Henkelman, A. Arnaldsson, H. Jónsson, J. Chem. Phys. 121 (2004) 9776–9792.
[56] B. Flemmig, I. Kretzschmar, C.M. Friend, R. Hoffmann, J. Phys. Chem. A 108 (2004) 2972–2981.
[57] T. Classen, M. Lingenfelder, Y. Wang, R. Chopra, C. Virojanadara, U. Starke, G. Costantini, J. Phys. Chem. A 111 (2007) 12589–12603.
[58] X. Pang, C. Wang, Y. Zhou, J. Zhao, G. Wang, J. Mol. Struct. Theochem. 948 (2010) 1–10.
[59] R. Szukiewicz, J. Kołaczkiewicz, I.N. Yakovkin, Surf. Sci. 602 (2008) 2610–2616.
[60] I. Filot, S. Shetty, E.J.M. Hensen, R.A. Santen, J. Phys. Chem. C 115 (2011) 14204–14212.
[61] N.Y. Yang, A.J. Medford, X.Y. Liu, F. Studt, T. Bligaard, S.F. Bent, J.K. Nørskov, J. Am. Chem. Soc. 138 (2016) 3705–3714.
[62] A.J. Medford, A.C. Lausche, F.A. Pedersen, B. Temel, N.C. Schjødt, J.K. Nørskov, F. Studt, Top. Catal. 57 (2014) 135–142.
[63] S. Amaya-Roncancio, D.H. Linares, H.A. Duarte, K. Sapag, J. Phys. Chem. C 120 (2016) 10830–10837.
[64] M. Zhuo, A. Borgna, M. Saeys, J. Catal. 297 (2013) 217–226.
[65] X.C. Sun, R.G. Zhang, B.J. Wang, Appl. Surf. Sci. 265 (2013) 720–730.
[66] R.G. Zhang, F. Liu, Q. Wang, B.J. Wang, D.B. Li, Appl. Catal. A: Gen. 525 (2016) 76–84.
[67] H.X. Liu, R.G. Zhang, L.X. Ling, Q. Wang, B.J. Wang, D.B. Li, Catal. Sci. Technol. 7 (2017) 3758–3776.
[68] H. Kirsch, X.H. Zhao, Z.F. Ren, S.V. Levchenko, R.K. Campen, J. Phys. Chem. C 120 (2016) 24724–24733.
[69] S.D. Jackson, B.J. Brandreth, D. Winstanley, J. Catal. 106 (1987) 464–470.
[70] W. Wang, Y. Wang, G.C. Wang, Phys. Chem. Chem. Phys. 20 (2018) 2492–2507.
[71] G.R. Wang, R.G. Zhang, B.J. Wang, Appl. Catal. A: Gen. 466 (2013) 77–89.
[72] P. Liu, A. Logadottir, J.K. Nørskov, Electrochim. Acta 48 (2003) 3731–3742.
[73] S. Shetty, R.A. Santen, P.A. Stevens, S. Raman, J. Mol. Catal. A: Chem. 330 (2010) 73–87.
[74] E.A. Carter, Science 321 (2008) 800–803.
[75] P. Huang, E.A. Carter, Annu. Rev. Phys. Chem. 59 (2008) 261–290.
[76] F. Besenbacher, I. Chorkendorff, B. Clausen, B. Hammer, A. Molenbroek, J.K. Nørskov, I. Stensgaard, Science 279 (1998) 1913–1915.
[77] B. Hammer, J. Nørskov, Surf. Sci. 343 (1995) 211–220.
[78] S.S. Sung, R. Hoffmann, J. Am. Chem. Soc. 107 (1985) 578–584.
[79] P. Hu, D.A. King, M.H. Lee, M.C. Payne, Chem. Phys. Lett. 246 (1995) 73–78.